AIAA 99-4948

An Airbreathing Launch Vehicle Design with Turbine-Based Low-Speed Propulsion and Dual Mode Scramjet High-Speed Propulsion

P. L. Moses, K. A. Bouchard, R. F. Vause, S. Z. Pinckney
FDC / NYMA, Inc., Aerospace Sector,
NASA Langley Research Center, Hampton, VA
and
S. M. Ferlemann, C. P. Leonard, L. W. Taylor lll,
J. S. Robinson, J. G. Martin, D. H. Petley, J. L. Hunt
NASA Langley Research Center, Hampton, VA

9th International Space Planes and Hypersonic Systems and Technologies Conference
and
3rd Weakly Ionized Gases Workshop
November 1-5, 1999/Norfolk, VA

AIAA-99-4948

AN AIRBREATHING LAUNCH VEHICLE DESIGN WITH TURBINE-BASED LOW-SPEED PROPULSION AND DUAL MODE SCRAMJET HIGH-SPEED PROPULSION

P. L. Moses, K. A. Bouchard, R. F. Vause, S. Z. Pinckney
FDC / NYMA, Inc., Aerospace Sector, NASA Langley Research Center, Hampton, VA

L. W. Taylor III, S. M. Ferlemann, C. P. Leonard, J. S. Robinson, J. G. Martin, D. H. Petley, J. L. Hunt
NASA Langley Research Center, Hampton, VA

Abstract

Airbreathing launch vehicles continue to be a subject of great interest in the space access community. In particular, horizontal takeoff and horizontal landing vehicles are attractive with their airplane-like benefits and flexibility for future space launch requirements. The most promising of these concepts involve airframe integrated propulsion systems, in which the external undersurface of the vehicle forms part of the propulsion flowpath. Combining of airframe and engine functions in this manner involves all of the design disciplines interacting at once. Design and optimization of these configurations is a most difficult activity, requiring a multi-discipline process to analytically resolve the numerous interactions among the design variables. This paper describes the design and optimization of one configuration in this vehicle class, a lifting body with turbine-based low-speed propulsion. The integration of propulsion and airframe, both from an aero-propulsive and mechanical perspective are addressed. This paper primarily focuses on the design details of the preferred configuration and the analyses performed to assess its performance. The integration of both low-speed and high-speed propulsion is covered. Structural and mechanical designs are described along with materials and technologies used. Propellant and systems packaging are shown and the mission-sized vehicle weights are disclosed.

Nomenclature

A/R	Airbreather / Rocket
ABLV	Air Breathing Launch Vehicle
ACE-TR	Air Core Enhanced Turbine Ramjet
AMHT	All Moving Horizontal Tails
AML	Adaptive Modeling Language
AOA	Angle of Attack
APF	Advanced Polyimide Foam
ATS	Access to Space
BSL	Boeing Company, St. Louis
CAD	Computer Aided Design
CFD	Computational Fluid Dynamics
CG	Center of Gravity
CTSC	Combination Turbine Scramjet Cycles
DOE	Design of Experiments
DOF	Degree of Freedom
DMRS	Dual Mode Ramjet/Scramjet
DW	Dry Weight
Gr/Ep	Graphite Epoxy
HTO	Horizontal Takeoff
HXRV	Hyper-X Research Vehicle
IMI	Internal Multiscreen Insulation
Isp_{eff}	Effective Specific Impulse
ISS	International Space Station
L/E	Leading Edge
LOX	Liquid Oxygen
OHR	Oxygen-to-Hydrogen Ratio
P&W	United Technologies Pratt & Whitney Division
PAI	Propulsion-Airframe Integration
PFA	Propellant Fraction Available
PFR	Propellant Fraction Required
POST	Program to Optimize Simulated Trajectories
psf	Pounds per Square Foot
RBCC	Rocket Based Combined Cycle
RCS	Reaction Control System
SCM	Shape Control Members
SOL	Shock on Lip
SSTO	Single-Stage-to-Orbit
TABI	Tailorable Advanced Blanket Insulation
TOGW	Takeoff Gross Weight
TPS	Thermal Protection System
VTO	Vertical Takeoff

Background

Single-stage-to-orbit (SSTO) space access and atmospheric cruise missions are the subject of expanding activity within the hypersonic community. Viable and practical airbreathing, hypersonic propulsion systems for these vehicles are a primary focus of these efforts. Over the past 15 years, the U.S. Department of Defense and NASA hypersonic programs have spent over $3 billion advancing the readiness of hypersonic technologies [1]. New advances in high-speed propulsion, propulsion-airframe integration (PAI), structures, materials, thermal management concepts, and advanced design methods have further contributed to readiness for design of such vehicles. This paper addresses the integration of these technologies into a viable HTO SSTO configuration. This configuration, as shown in Figure 1, is a lifting body with

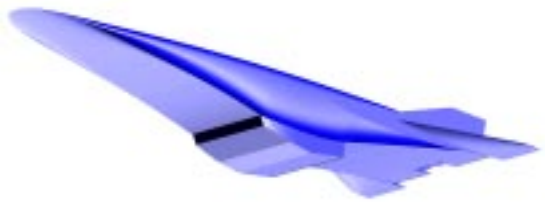

Figure 1. Horizontal-Take-Off, Single-Stage-To-Orbit, Airbreathing Launch Vehicle with Airframe-Integrated Propulsion Systems

an airframe-integrated, airbreathing propulsion system.

NASA's Access-To-Space (ATS) Study revealed one promising configuration within the configuration matrix, for an HTO SSTO mission with 25,000 lb. of payload [2]. Payloads of this class are required to service the International Space Station (ISS) in a 220 N.M. orbit at 51.6° inclination. The configuration that appears most promising for HTO SSTO mission is the lifting body with an airframe-integrated, dual mode ramjet/scramjet (DMRS) high-speed propulsion. Further refinement of this configuration and the exact nature of multi-mode propulsion required for this mission are objects of NASA's current AirBreathing Launch Vehicle (ABLV) Study. This configuration also requires a low-speed propulsion system to get off the ground and accelerate to the ramjet take-over speed, as well as some form of rocket and/or LOX augmented propulsion to transit from atmospheric to exoatmospheric operation. Several configurations and propulsion systems were examined for HTO SSTO using the ISS mission in the current study. These included winged-bodies, conical vehicles, high-fineness vehicles, podded engine concepts, and lifting bodies. From this effort, the lifting body configuration stands out as having potential for development to meet the demanding HTO SSTO mission.

The single most critical technology for such vehicles is the high-speed propulsion system, which is the dual mode ramjet/scramjet (DMRS). Recent progress in this area is illustrated by NASA's Hyper-X Program, where autonomous, powered and unpowered flight at Mach 7 and 10 will soon be demonstrated. The Hyper-X Research Vehicle (HXRV) or X-43 will be boosted to the test conditions by a Pegasus based booster, separate from the launch vehicle, and perform the hydrogen fueled propulsion test in free flight [1]. This research vehicle is highly significant to the space access mission because the configuration, as shown in Figure 2, is very similar and employs the

Figure 2. Hyper-X Research Vehicle with Airframe-Integrated, Dual Mode Ramjet/Scramjet Propulsion

same type of DMRS high-speed engine with similar airframe integration. Ground tests with a full-scale, X-43 flight engine have already demonstrated operability and performance at or above predicted levels, in the 8' High Temperature Tunnel at NASA Langley Research Center. Combining this efficient high-speed propulsion technology with appropriate choices for the remaining propulsion modes is the key to creating an efficient configuration for HTO SSTO.

Introduction

Reference Vehicle - ABLV Study

In the performance of a system study for configuration development and propulsion system trades, it is imperative to have a good baseline con-

figuration or reference vehicle. This vehicle should be relatively well characterized and be compatible with the configuration and propulsion systems to be compared. The maturity of the reference vehicle design and analyses must be such that the sensitivity to a given technology will be evident when it is installed. If the reference design is poorly substantiated, changes in propulsion technology may not show significant impact to the vehicle. Likewise, the level of analytical effort applied to characterize a new propulsion system must be compatible with efforts applied to the reference vehicle. In the ABLV Study, the reference vehicle chosen for comparison of configurations and propulsion systems was an updated version of the Airbreathing / Rocket SSTO configuration of the ATS Study [2]. This reference vehicle, ABLV-4, is a lifting body with a fineness ratio of about 5.6, as shown in Figure 3. Through-

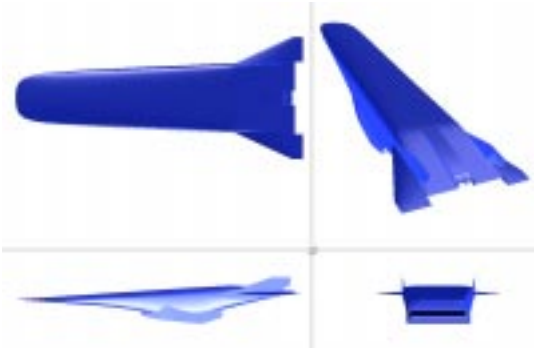

Figure 3. ABLV-4 Reference Vehicle - HTO SSTO Mission to International Space Station

out this paper, configuration numbers will be used to refer to various vehicles from the ABLV Study. They are simply a numerical designator with no other significance. The reference vehicle employs the same propulsion system arrangement as used in the ATS Study. ABLV-4, is a cold, integral-tank architecture, with advanced thermal protection systems (TPS) and is fueled with slush hydrogen (50% solids / 50% liquid). The thick sidewalls, which housed the novel main landing gear installation, impose substantial drag penalties on the vehicle and as the size of the vehicle increases, the landing gear installation becomes a greater risk. Finally, there is a concern that the reference vehicle has too low a fineness ratio (relatively blunt configuration) and may be imposing higher drag losses than necessary. The reference vehicle, ABLV-4, is currently closed at a TOGW of about 1.07×10^6 lb., without addressing the risks/issues explained above. The work reported in this paper seeks to address these issues and mitigate the risks through appropriate design changes, during development of the preferred airbreathing HTO SSTO configuration, with turbine-based low-speed/DMRS high-speed propulsion systems in an over/under integration.

Figure of Merit

The design of an airframe-integrated propulsion system and hypersonic vehicle is a very complex process, involving numerous physical interactions and requiring a multi-discipline approach. How then, does the vehicle designer determine a figure of merit to measure propulsive efficiency? The answer has both simple and complex parts. The simplest figure of merit to demonstrate propulsive impact on a vehicle is the “closed” vehicle’s takeoff gross weight (TOGW) or dry weight (DW). A closed vehicle is defined as having the exact propellant fraction available (PFA) to deliver the propellant fraction required (PFR) of the mission, or simply PFA=PFR. The choice between TOGW and DW is complex because DW typically drives initial cost more heavily, while TOGW drives operational cost and life-cycle-cost (including infrastructure) heavily. At the conceptual level of these studies costs are not yet being addressed, so minimum TOGW was chosen as the figure of merit.

The complex part of this “propulsion assessment” comes from the level of design and analysis effort required to credibly compare a series of propulsion systems integrated to the same configuration. Characterization of airbreathing, hypersonic vehicle performance is a multi-discipline process, requiring interaction of the design and analysis disciplines to an unparalleled extent. Figure 4 illus-

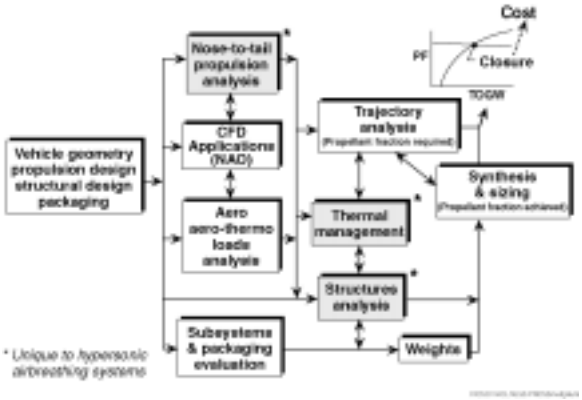

Figure 4. Design / Analysis Process for Hypersonic Airbreathing Vehicles

trates the level and type of interactions required to resolve vehicle performance, with numerous competing design variables that must be evaluated.

Propulsion System Selection

With minimum TOGW as the goal, various multi-mode propulsion systems were examined by integrating them to the reference configuration for the HTO SSTO mission. The choices considered fell into three potential arrangements of combined cycles (one flowpath, multiple modes) and combination engines (multiple flowpaths, multiple modes). The reference arrangement was an air-breather/rocket system like the A/R SSTO vehicle of Option 3 from the ATS Study[2], which was used for reference only and not discussed here. The second propulsion arrangement studied, was rocket-based-combined-cycle (RBCC), in which a single flowpath functions in all modes from low-speed, to high-speed, to pure rocket. The third propulsion arrangement was a combination of engines and cycles with turbine-based low-speed, DMRS high-speed, and external tail rocket. The combination of turbine-based and DMRS was designated Combination Turbine Scramjet Cycles (CTSC) and is the principle focus of this paper.

Selection of propulsion cycles for integration into a vehicle requires consideration of all impacts to the vehicle. One aspect of these considerations is the amount of liquid oxygen (LOX) required to be carried by the vehicle. LOX is a very dense fluid and will increase average propellant density rapidly as increasing quantities of LOX are carried with the low density hydrogen fuel. This can have the impact of increasing structural weight to carry greater loads and increasing the planform loading, which will increase takeoff speeds of the lifting body configuration. These distinctions for vehicles carrying higher LOX fractions led to the consideration of propulsion cycles that emphasized air-breathing and minimized LOX usage.

Among those cycles requiring less LOX are the turbine-based machines such as the Pratt &Whitney (P&W) Air-core-enhanced Turboramjet (Ace-TR), a proprietary, high thrust-to-weight, turbine based engine. This engine is one example of advanced turbine-based systems that are projected to deliver uninstalled thrust-to-weight (T/W) ratios between 16:1 and 24:1. The early goal for uninstalled T/W ratio of the turbine-based system was 24:1, but this was later dropped to 20:1 to reflect more near term technology. The higher T/W was used to make initial predictions of this type engine's impact on the configurations studied, but the final configuration closure evaluated reducing the uninstalled T/W to 20:1. Combining this type engine with the DMRS high-speed system in an over/under arrangement appeared to be the best airframe integration to study. To gage the potential of this low-speed system integration, a derivative of the reference vehicle was developed with the Ace-TR low-speed engine, designated ABLV-4B, as shown in Figure 5.

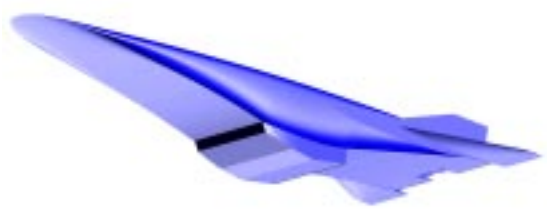

Figure 5. ABLV-4B, Airbreathing Launch Vehicle - CTSC and Rocket Propulsion

The Ace-TR low-speed integration was jointly designed with the Boeing Company - St. Louis (BSL), where the installed low-speed performance was generated. This vehicle was closed at 1.04×10^6 lb. TOGW, with the same landing gear integration as the reference vehicle, but using triple-point hydrogen fuel. Thus, the first comparison to the reference vehicle was favorable, but the other issues with the reference vehicle were still present. A decision was made to develop a second CTSC configuration with the main landing gear integrated into the fuselage and a somewhat higher fineness ratio to reduce drag.

Configuration Development

Concept Definition

The remainder of this paper will focus on the status of the design for a new CTSC vehicle and the design/optimization process employed. This process will be illustrated with the selected configuration, but issues with prior configurations will be addressed as they are resolved in the new vehicle. The prior CTSC configuration, ABLV-4B, had relatively high drag through the transonic region, which drove the decision to adopt a slightly higher fineness ratio relative to the reference vehicle. A similar configuration was developed with a fineness ratio of 6.9 as compared to the reference vehicle at

5.6. A detailed geometry sized to 120,000 ft^3 was prepared for analysis and designated ABLV-9, as shown in Figure 6.

Figure 6. ABLV-9 CTSC Configuration - 20% Higher Fineness Ratio than ABLV-4

Initial results for this configuration indicated that a shock-on-lip (SOL) Mach number of 12 would improve performance. This resulted in a new configuration with Mach 12 SOL, designated ABLV-9B. Maintaining consistent forebody and nozzle shapes enabled the design team to move ahead with the existing ABLV-9 geometry for development of structural concepts and packaging (internal subsystems arrangement). When vehicle geometry became available for the ABLV-9B keel line, the volume and surface area distributions of ABLV-9 would be adjusted to reflect ABLV-9B values, so that weights and propellant fraction available (PFA) from the synthesis model would be corrected to the new geometry.

The cold integral-tank architecture using graphite/epoxy (Gr/Ep) composite material was retained, due to its high efficiency. This efficiency results from two characteristics. The first is the very high specific strength and specific stiffness of the Gr/Ep material. The other is the high volumetric packaging factor for propellants, due to the conformal nature of the tank. An added contribution to the efficiency comes from the relative thinness of the advanced cryo-insulation and TPS. This is illustrated in Figure 7, which shows that a hot, non-integral-tank concept packages less fuel for the same cross-section. The nose of the vehicle is a carbon-carbon composite structure with an actively cooled leading edge (L/E). The control surfaces are twin vertical tails with rudders and twin all-moving-horizontal-tails (AMHT), which are a hot structure concept with passively cooled L/E. The structures will be more fully described in a later section. The

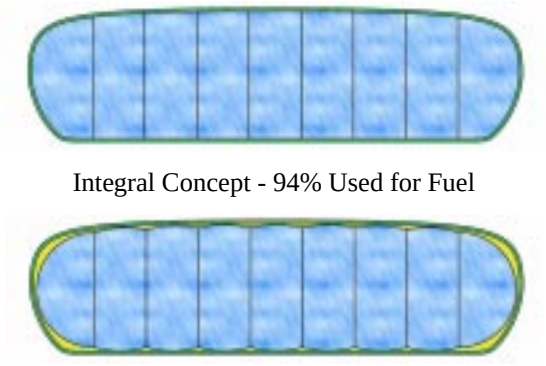

Figure 7. Comparison of Cold Integral Tank Concept with Hot Non-Integral Tank Concept

ABLV-9 configuration, compared to the ABLV-4 reference vehicle, has the increased fineness, reduced body width, and smaller sidewalls.

Geometry Definition

Geometry definition starts with the mission requirements. Horizontal or vertical orientation for takeoff and landing are major considerations that drive shaping and landing gear location. Shape is impacted by many competing considerations, such as propulsion capture area, payload packaging, and minimized aerodynamic drag. Thus, a clear and well defined mission is required to start configuration development. The mission, cost targets, and technology goals help to set ground rules for the design, including minimum included angles, thermal protection systems, structural concepts, fuel and oxidizer, crew, payload, gear, reusability, materials, maximum takeoff speed, cruise range, and others. The HTO SSTO mission with maximum airbreathing propulsion is a demanding design challenge. Relatively slender lifting bodies with airframe-integrated propulsion have proven an effective choice for hypersonic missions. The lifting body configuration is primarily driven by design of the high-speed airbreathing flowpath. The flowpath is composed of the entire undersurface of the vehicle, including forebody inlet ramps, centerbody engine with matching cowl, and aftbody nozzle surfaces. The first step is definition of a 2D keel line (longitudinal shear view). This design process is iterative in nature, requiring performance computations to determine when acceptable 2D operability and performance have been achieved. This process is aided by a modeling tool generated with Adaptive Modeling Language (AML) software [3]. The AML

tool is used for initial geometry construction and 2D propulsion analyis input deck generation. After an acceptable flowpath is defined, a three-dimensional vehicle geometry is wrapped around the extruded and trimmed 2D flowpath, using the Pro/ENGINEER computer-aided-design (CAD) tool [4]. This configuration forms the basis for packaging, thermal management, and structures discipline efforts.

The new configuration will be ABLV-9B and will follow the same geometry design process as the original configuration. In general, the fuselage must be shaped and sized to enclose required payloads and fuel/oxidizer volumes. The objective is to create, as closely as possible, a two-dimensional inlet for uniform flow into the engine and uniform flow onto the external nozzle from the engine exhaust. Design rules are followed for minimum included angles for cowl, sidewalls, and fuselage nose. Sidewall thickness for the ABLV-4 series of configurations was driven by the novel main landing gear installation, but for the ABLV-9 series the gear was moved into the fuselage volume. The aftbody side surfaces provide a flat wiping plane for the AMHT. Vertical control surfaces are fixed with trailing edge rudders. Linear aerospike rockets are integrated into a bump on the aftbody upper surface. This rearward bump location is shadowed from forebody flow and provides volume to package rocket systems. The lower aftbody nozzle surface is trimmed for the rocket nozzles. This first geometry is referred to as the “as-drawn” vehicle.

Vehicle Configuration Control

When the as-drawn vehicle is complete, aerodynamics, packaging, computational fluid dynamics (CFD), thermal management, structures, and other disciplines begin their analyses using models derived from these master surfaces. It is imperative that all disciplines are working the same configuration geometry (configuration control) or at least, fully understand any disconnects accepted in the process. If great care is not exercised in configuration control, closures can have significant errors. With a common configuration database, data can be shared confidently between disciplines, using common coordinate systems and known assumptions that are referenced to a single vehicle. After the as-drawn vehicle analysis is completed and trajectory simulation performed, closures may be performed to produce an “as-flown” vehicle. If the as-flown vehicle does not meet mission requirements, revisions may be made to address performance problems. This is a negotiated process among the design disciplines that requires compromise and concession to yield an improved configuration. Revised configurations are analyzed and the process is repeated until a satisfactory closure is obtained and the as-flown vehicle meets all requirements.

Trajectory Analysis

Analysis and Modeling

For this study, the vehicle mission is the insertion of a 25000 lb. payload into a ISS orbit (220 N.M. circular orbit, 51.6 degrees inclination). The trajectory and vehicle optimization were completed using the 3-Degree of Freedom (DOF) Program to Optimize Simulated Trajectories (POST) [5]. Trajectory simulations were performed with the vehicle aerodynamically trimmed in the pitch plane. The goal of the trajectory optimization is to perform the mission for the minimum vehicle TOGW. A closed vehicle’s TOGW is determined by inputting the mission PFR and propellant LOX fraction, from the trajectory analysis, into the vehicle closure model. The closure model is more fully described in a following section. The closure model then scales the as-drawn vehicle to a size and weight that match the trajectory requirements. Using the vehicle closure model, a table of TOGW as a function of PFR and LOX fraction was generated and imported into the POST simulation as the optimization function. This provides the optimizer with a direct impact on TOGW as it trades thrust and Isp levels for the various propulsion systems, as well as varying other parameters. Figure 8 describes the trajectory in terms of altitude versus Mach number and illustrates the various segments of the trajectory characterized by each propulsion mode.

Propulsion Modes

A typical airbreathing hypersonic vehicle operates in multiple engine cycles and the CTSC integration is no different in that respect. In low-speed (Mach 0-4) the vehicle is powered by a bank of Ace-TR engines, which themselves have multiple cycles/modes (subsonic turbine operation, supersonic turbine/ramjet operation). This mode transition is transparent to the trajectory design because the engine operation and performance are represented purely by a single matrix of thrust and propellant flowrate, as functions of Mach number and angle of attack (AOA). Also in this Mach range, the

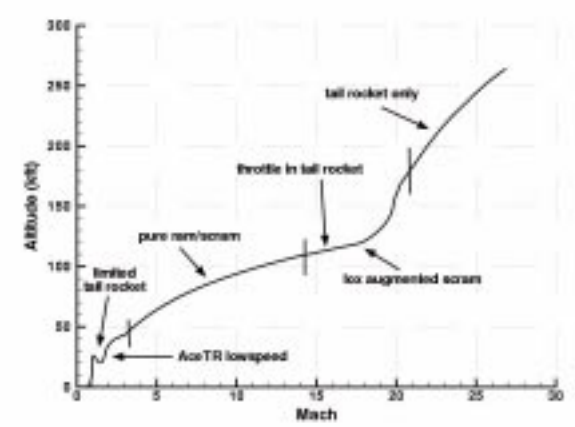

Figure 8. Trajectory Altitude vs. Mach Number - Ranges of Propulsion Mode Operation

optimizer is given the option of using the linear aerospike tail rocket for additional thrust. This is generally the case at takeoff and in the transonic region, where the vehicle drag increases significantly and additional thrust is usually required to accelerate through and beyond Mach 1.

The next propulsion mode is main engine ramjet/scramjet operation. Again, the transition from ramjet to scramjet mode is accounted for in the data table and is transparent to the trajectory optimization. Following pure scramjet operation, a mix of LOX augmented scramjet and tail rocket operation is employed. Here, the optimizer trades the high Isp of the pure scramjet for a higher thrust of the internal LH_2/LOX rocket motors firing into the main flowpath in the LOX augmented mode. The optimizer again has the option of using the tail rocket as necessary. It is during this mode that the pull-up maneuver usually occurs, requiring high thrust and necessitating the use of the tail rocket. During the pull-up, when the dynamic pressure falls below the level that will sustain main engine combustion, the main engine is shut down and the vehicle relies solely on the tail rocket for the remainder of the flight.

Although there are several propulsion mode transitions that are transparent to the trajectory optimization, there are several that play key roles in reducing the vehicle's TOGW. The Ace-TR system requires a substantial amount of variable geometry, especially in the Mach 3.5 and higher range. The required amount of variable geometry directly impacts the weight and volume of the system, effecting the entire vehicle's size and weight. Thus, the transition Mach number from Ace-TR to high-speed engine operation plays an important role in the overall vehicle optimization. The trade-off for lowering this transition Mach number comes in a potentially larger ramjet to deliver added low-speed thrust and reduced performance by the scramjet engine in the higher Mach range (above Mach 12). This optimization is not addressed by the current effort. The second transition that the optimizer uses is the switch from pure scramjet to LOX augmented scramjet operation. The optimizer is also given control over the oxygen-to-hydrogen ratio (OHR) of flowpath rocket motors. In addition, the optimizer may again use tail rocket as required. It also has indirect control of when to shut off the main engine by moving the pull-up Mach number (recall that the main engine is shut off at a limiting dynamic pressure).

Guidance

In addition to the aerodynamic and propulsive characteristics of the vehicle, the simulation tool requires a guidance scheme(s) in order to simulate the trajectory. The guidance schemes employed must be compatible with the vehicle design and mission requirements. Figure 9 shows trajectory

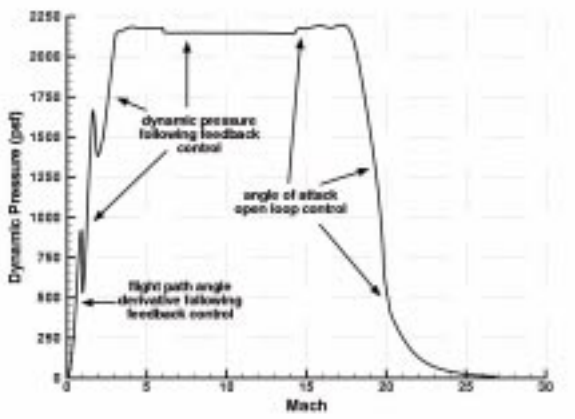

Figure 9. Trajectory Dynamic Pressure vs. Mach Number - Ranges of Guidance Schemes

dynamic pressure versus Mach number and illustrates where various guidance schemes are operative, as described below. In the first phase of the flight, the guidance routine follows a flight path angle derivative profile (with respect to time), controlled by the optimizer. After the vehicle has established supersonic flight, the guidance scheme

switches to a dynamic pressure following routine. The cruise dynamic pressure for this vehicle is generally around 2000 psf. Again, this profile is controlled by the optimizer. This guidance mode takes the vehicle up to the point where the optimizer decides to augment the main scramjet with LOX augmented scramjet performance or switch to pure tail-rocket thrust. From this point forward (until orbit insertion), the vehicle is controlled by an AOA profile as a function of Mach number, again controlled by the optimizer.

Optimization

In summary, the optimizer has control over the following parameter profiles: low speed and high speed tail rocket throttling tables, a flight path angle derivative table, a dynamic pressure table, and a pull-up AOA table, all as functions of Mach number. This optimization process typically results in 30-40 independent variables for the optimizer to control, depending on the size of the tables. Additionally, constraints are added from the various disciplines. Structural constraints impose a normal acceleration limit of 2.5 g's and a total acceleration limit of 4.0 g's. Thermal restrictions limit the maximum dynamic pressure to 2200 psf., as well as limiting the AOA to less than 5 below Mach 18 and less than 8 above Mach 18. In the LOX augmented scramjet mode, the OHR is limited to between 1 and 6. Also, as stated earlier, propulsive operability dictates that the scramjet engine be cut off at 200 psf. dynamic pressure.

Aerodynamic and Aerothermodynamic Performance

The aerodynamic database can be split into two distinct pieces: low speed and high speed. The reason for the division lies in the methods used to calculate the aerodynamic phenomena. The high speed portion of the database corresponds roughly to speeds greater than Mach 3. At these velocities, lift and drag are modeled successfully by engineering codes such as APAS [6] and SHABP [7] for arbitrary configurations. For these programs, the inviscid pressure forces are predicted by impact and shadow methods such as modified newtonian, tangent cone, tangent wedge, and Prandtl-Meyer expansions. However, for compression surfaces careful attention must be paid to the initial flow conditions for increasing angle surfaces as flow moves downstream. Skin friction results are generated through reference temperature and reference enthalpy methods. Engineering codes are powerful design tools in the conceptual design stage. Their use in the early stages of design enables higher level CFD and wind tunnel analyses to be performed on more mature vehicle concepts. CFD and experimental work can also be used to capture flow features, such as flow separation regions, which may not be predicted by lower order methods.

Low speed aerodynamics are more difficult to obtain in part due to the strong nonlinear aerodynamics associated with hypersonic lifting body configurations. Solutions for arbitrary shapes are not readily available and higher order methods must often be used to achieve adequate fidelity. For this reason, the low speed aerodynamic database is anchored to an historical database for a similar configuration. The historical database was created from a combination of engineering code, CFD, and wind tunnel testing for a very similar configuration. A limited number of higher order analyses can then be used to tailor the historical database to the present configuration.

Because of the nature of an airframe-integrated scramjet powered vehicle, the distinctions between traditional aerodynamics and propulsion become blurred. The entire lower surface of the vehicle becomes part of the engine flowpath. Determining which discipline should be responsible for which areas on the vehicle is critical. Great care must be taken when accounting for forces and moments on the vehicle. For the class of vehicle described in this paper, cowl-to-tail accounting is used. Cowl-to-tail accounting gives the forebody, upper surface, chines, external engine sidewalls, wings, tails, and wiping planes to the aerodynamics discipline, while the external cowl, engine internals, and nozzle are totaled in the propulsion forces and moments.

Aerothermal load generation on vehicle acreage is well modeled through Reynold's analogies for ideal or real gases using codes such as APAS and SHABP. Blunt body heating can be solved through the use of other codes such as StagHeat, an in-house engineering program, which employs adjusted Fay-Riddell correlations for ideal or real gases. While these methods cover the majority of the vehicle surface, airbreathing configurations have particular thermal challenges. Shock-shock interactions on the engine cowl leading edge, corner flows such as the vertical tail/AMHT junction, and gap heating between the AMHT and vertical tail are phenomena which can easily increase the

predicted heating by an order of magnitude. Quantifying the heat augmentation is difficult because it is heavily configuration and attitude dependent. For this reason, multipliers can be obtained from literature surveys for similar configurations and applied to heat loads for initial thermal analyses, but should be verified through wind tunnel testing or other means.

Propulsion System

Low-Speed System

The low-speed system selected for initial study was the P&W Ace-TR, a proprietary development of the Pratt & Whitney Aircraft Engine Company. For this reason, the specific design details and performance parameters are not disclosed in this paper. Because it provides a good example of advanced turbine engines, the P&W engine cycle performance was used in computing the installed performance of the system. However, other turbine-based engines will be considered in the future. Figure 10 shows the installation of this

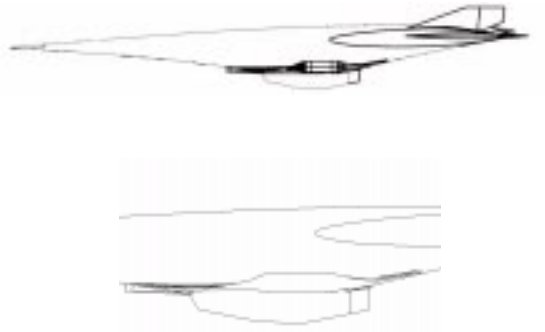

Figure 10. Ace-TR Low-Speed System Integration - Shear View

engine, as applied to the ABLV-9 configuration. Six of these engines were installed in the ABLV-9 configuration, with three 2-D common inlet and nozzle structures serving each pair of Ace-TR engines, as shown in Figure 11. Each engine is served by its own rectangular-to-circular transition section that is split off the common 2D inlet or nozzle. This arrangement was chosen to integrate compatibly with the three high-speed engines, which each have two side-by-side flowpaths, for a total of six. Because of structural integration requirements with the airframe, the six Ace-TR engines are evenly spaced across the vehicle, on-center with the high-

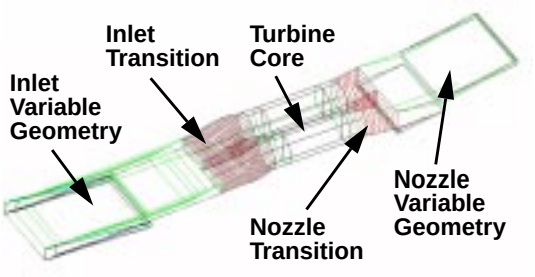

Figure 11. Ace-TR Low-Speed System Integration - 2D Inlet and Nozzle with Transitions

speed flowpaths. This will allow for similar servicing and installation procedures for both low-speed and high-speed engines.

Development of this installation was a joint effort between NASA LaRC, P&W, and BSL. P&W supplied BSL with the Ace-TR engine airflow demand curve and Boeing designed the inlet to meet that demand. The engine analysis performed at BSL accounted for inlet operability and performance using 2D methods. Operability issues are a key element of the design, since the variable geometry inlet must receive supersonic flow and supply subsonic flow to the Ace-TR, with relatively low distortion. For this reason, an isolator/subsonic diffuser must be designed that is long enough to produce subsonic flow across the entire Mach number range of the low-speed system. The inlet recovery developed at BSL was used in a P&W Ace-TR cycle deck (computer code) to get installed engine performance. The nozzle characteristics are relatively well known, so the installed performance can be computed using an estimated nozzle gross thrust coefficient (CFG).

High-Speed System

As previously described, ABLV-9B is a Mach 12 SOL version of the ABLV-9 configuration. Development of the Mach 12 keel line geometry started with an extension of the existing, final forebody ramp to make the engine deeper. Several values for the inlet final ramp length were investigated to produce a cowl inlet length that was somewhat shorter than the ABLV-4 cowl inlet. A matrix of propulsion performance computations was made and tabulated as functions of Mach number, angle of attack, and dynamic pressure. Also included were cases for LOX augmented scramjet performance. These data were then utilized in the POST trajectory optimization and vehicle performance assess-

ment. Thus, the closures generated for the ABLV-9B vehicle will be made with appropriately computed data, from the 2D performance code. While 3D effects on propulsion are a concern, the assessment would be premature at this stage of design. When making multiple trades of propulsion systems in a study, an exhaustive CFD study is unwarranted in terms of cost and time. As long as the configurations are similar, as they are for the current study, the 3D impact will not be a discriminator. If two promising systems were to be nearly identical in performance, then an assessment for 3D effects may be in order, but only if the 2D performance showed potential in the vehicles.

External rocket

The external rocket system utilized on these configurations was a linearized version of the aerospike rocket engine concept. This engine concept integrates small rocket combustors around an annulus exhausting over an axi-symmetric nozzle. The linearized version of this technology unwraps the annular combustor arrangement into a 2D arrangement, with symmetric upper and lower combustors exhausting over a symmetric 2D nozzle, as shown in Figure 12. The upper and lower

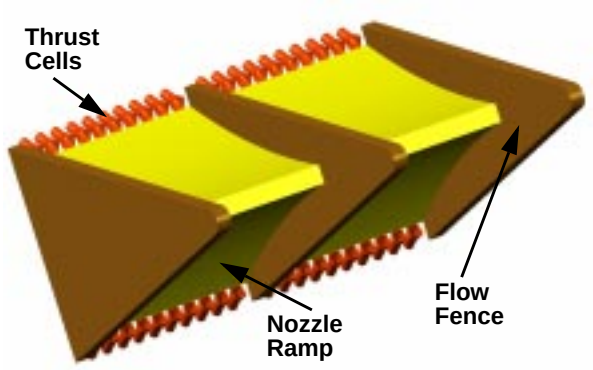

Figure 12. Linear AeroSpike Rocket Engine Integration in Tail Section of Vehicle

sections are broken into a number of independent segments that are arranged across the width of the engine. The installation of the tail rocket is oriented to place its thrust vector through the CG of the vehicle. In addition, each segment is independently operable and “throttleable”, giving the ability to produce asymmetric thrust for trimming or control of the vehicle. This capability is in addition to the vehicle’s reaction control system, which is designed primarily for exoatmospheric operation. With all segments in operation, the gross thrust is 270,000lb at 458 sec. Isp (vacuum). This rocket technology was predicted to deliver a goal thrust-to-weight ratio of 77:1, which is used to obtain the scaled rocket weight in the synthesis model.

Structure

Structural Concepts

The structural concept used for the ABLV vehicle is shown in Figure 19. Surface panels transfer airload and propulsion pressures to an underlying grid of longitudinal keel beams and transverse bulkhead beams. Longitudinal bending moment is carried primarily by the top and bottom skins with the keel beam webs reacting the associated transverse shear. In areas where the skin panels are discontinuous (payload and engine compartments), longitudinal bending is resisted by couple forces in the top and bottom caps of the keel beams. The transverse bulkhead beams carry shear and bending in the inboard-outboard direction and also function to reduce the buckling length of compression-loaded skin panels. Bulkheads are also important in distributing concentrated loads such as landing gear forces. Between bulkheads are panels designated as shape control members (SCM) which function in pressurized compartments to limit skin lateral displacements. In addition to aerodynamic concerns, lateral skin displacements must be minimized to prevent in-plane loads from generating additional skin bending moments. Surface loads on the horizontal are carried by a skin-spar system with the tapered spars originating at the spindle attachment. The vertical control surface is also formed with a skin-stiffener system. This structural concept is exceedingly stiff and can carry axial load, bi-directional bending, and torsion very efficiently.

The planned upgrade to structural sizing methodology is described in the following sections, but is not yet fully functional. The major advantage to this process is that it is a “bottoms-up” analysis and sizing for the actual airframe loads. It will not require a vehicle density correction factor for increased LOX load. Unfortunately, other demands have prevented completion of this effort. Therefore, the unit weights and structural methodology used in the closure model remain the same as for the reference vehicle, ABLV-4. However for these vehicles, the LOX fraction stayed near the reference value and planform loading never exceeded the takeoff limit. Thus, the density correction factor on

structure and takeoff penalty were never an issue for these vehicles. While the absolute values of weight may have some uncertainty, the relative trends will be correct.

Structural Geometry and Elements

Initial ABLV surface geometry was very detailed in order to be suitable for aerodynamic modeling. In order to predict structural unit weights, a simpler geometry definition was needed to generate an internal structure and to obtain quick estimates of lengths, surface area, volume, and mass properties. The base structural geometry was created by passing planes through the original model at selected bulkhead stations (Figure 13). The

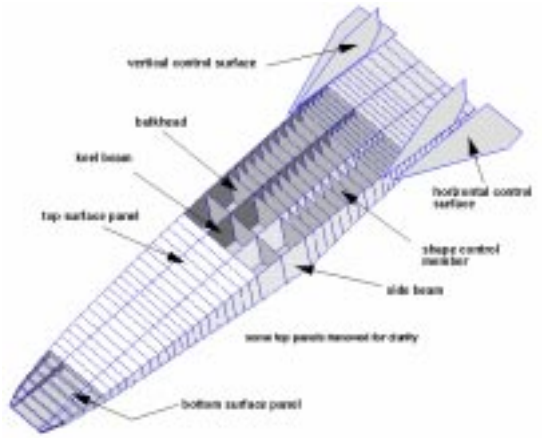

Figure 13. Structural Arrangement

planes are located where the geometry changes abruptly or where concentrated loads will be applied to the vehicle structure. A simplified cross-section provides reference points for calculating cross-section width, depth, and center of gravity. All external and internal structural elements are generated from the base cross-section geometry. Bulkheads are located at the base cross-section stations while the spacing of intermediate shape control members and keel beams can be varied in the geometry generating code. The initial ABLV geometry and a simplified structural geometry are shown in Figures 14 and 15 . The elements shown in Figure 15 are actually a NASTRAN model written by the geometry generator.

The structural elements which are tracked in the sizing and weights procedure are shown in Figure 16. Keel beams, bulkhead beams, and side beams are all formed from webs and flange caps.

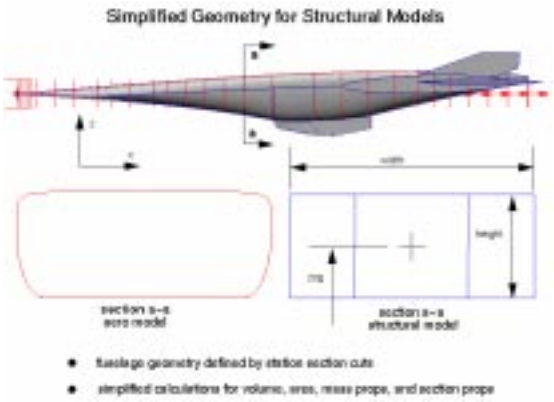

Figure 14. Simplified Geometry for Structural Models

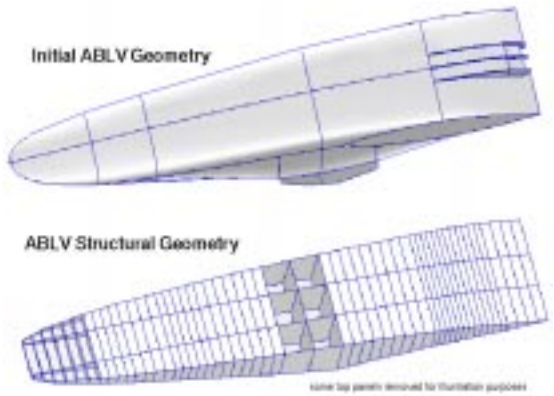

Figure 15. Structural Geometry

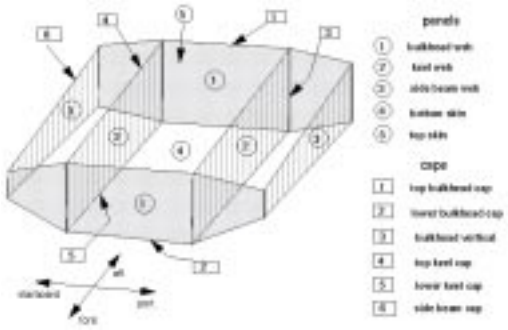

Figure 16. Section Structural Members

The beam caps carry axial and bending loads (couple force) while the webs mainly resist shearing loads. The skin panels are shown as a simple planar structure but these elements are assigned a skin-stiffener arrangement in the sizing procedure to generate appropriate membrane, bending, and

shear stiffnesses at the modeled reference surface. A single solid element is generated within each compartment to simplify mass distribution for the model.

Structural Loads and analysis

Structural load cases for the ABLV HTO SSTO vehicles are tied closely to points on the trajectory analysis. Initial load cases are based on trajectory points for maximum axial acceleration, maximum normal acceleration, and the maximum vector combination of axial and normal accelerations. Also associated with the trajectory load case points are integrated airloads, integrated propulsion loads, accelerations, and control surface trim loads. Pressure distributions for high-speed airloads and propulsion loads are defined by engineering aerodynamic codes and engine performance codes. However, maximum vehicle bending loads often occur during a pull-up maneuver at low speed (less than Mach 3). Airload and propulsion pressure distributions at low speeds are usually not well defined during the early stages of systems analysis and integration. Pressures on the engine ramps and nozzle are important to panel design, as well as to overall shear and bending of the fuselage structure. For low speed cases, approximate pressure distributions on the lower forebody and nozzle areas were generated from trajectory forces and moments. Aerodynamic normal force and reference pitching moment were used to solve for a pressure distribution with constant and quadratic terms. Axial aerodynamic force was matched using the force component from the ramp pressures and a drag contribution from the vehicle upper and side surfaces. Nozzle pressures also use constant and quadratic terms based on propulsion moment and thrust requirements. The vehicle free body with relevant pressure distributions is illustrated in Figure 17. The distributed pressures are applied to the ramp and nozzle panels and then combined with other forces to check for dynamic equilibrium. The accelerations solved for using the distributed pressures are compared to accelerations from the trajectory analysis. Good agreement between the two measures of acceleration are required before the load case definition proceeds.

Loads on the surface panels are mapped to a line model at the center of a station segment as seen in Figure 18. This procedure replaces all surface loads with an equivalent set of loads on a line

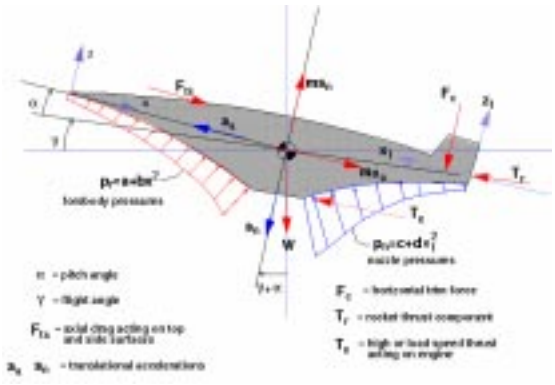

Figure 17. Vehicle Free Body for Flight Loads

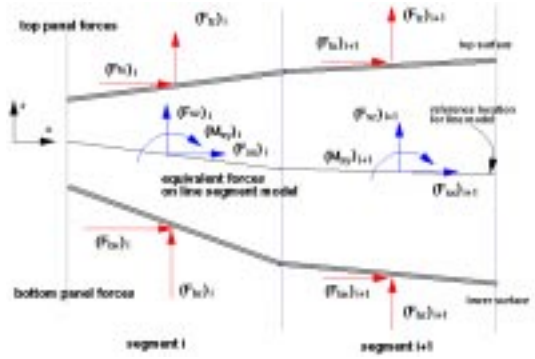

Figure 18. Equivalent Segment Loads for Line Model

model which extends from nose to tail. A similar procedure is used for mapping the distributed inertial loads to the line model. Checks are made to verify that the distributed loads on the line model produce the same set of integrated forces that were used in the trajectory analysis. The line model should be in dynamic equilibrium under a combined set of airloads, propulsion loads, inertial loads, and control surface loads. Internal axial force, shear force, and bending moment at any station point can be determined from standard equations. Repeating this procedure for the chosen load cases produces a useful set of internal force envelopes. Panel pressures and forces can also be written to the NASTRAN model shown in Figure15 for a finite element analysis. The inertia relief capability of NASTRAN is used to solve for inertial loads which will be in equilibrium under applied airloads, propulsion loads, and control surface loads. Loads development was tightly integrated through all three levels of structural modeling for ABLV. Consistency was maintained when moving from a

lumped mass and force trajectory model to a distributed mass and force line model or three-dimensional panel and beam model.

Structural Sizing

Internal forces from the line models described above are used for first order structural sizing of the central tube formed by the skins and keel beams. Graphite-epoxy stiffness values and strain allowables are used with the applied forces to calculate required section thicknesses, using classical engineering methods. Beyond the first order prediction described above, formal sizing of the structural elements may be carried out with the HyperSizer code from Collier Research Corporation [8]. Specific HyperSizer cross-sections and materials are assigned by the user to all panel and beam element groups. HyperSizer's material library includes composites and metals and the range of panel cross-section types includes sandwich sections, hat-stiffened sections, biaxial blade stiffened sections, and grid-stiffened sections. Beam cross-section types include most open and closed sections common to aircraft construction. Within each cross-section description are a group of variables such as stiffener width, depth, and spacing. The user assigns realistic ranges to each of the design variables. HyperSizer submits the job to NASTRAN for the load cases described above. Internal membrane and bending forces are then passed back to HyperSizer, which chooses the cross-section variables that produce the lowest section weight and satisfy all strength and stiffness criteria. Updated NASTRAN stiffnesses can be written out to see the influence of the new section stiffnesses on load distribution. If there are significant changes in load distribution, then additional iterations of the analysis cycle are performed with the new load distribution and revised stiffnesses until the process converges (output weights don't change).

Structural Weights

The structural weights determined by analysis are summed up for each section of the structural model. (Recall that the structural geometry is a close approximation of the actual vehicle geometry.) Structural unit weights for each section of the structural model are generated using lengths and surface areas of the model. These unit weights are passed to the synthesis tool for integration over the actual geometry of the configuration, insuring that all parts of the real geometry are assigned realistic unit weights. Recall that the status results are still for the ABLV-4 structural unit weights.

Thermal Management

Thermal Protection Systems

A thermal protection system (TPS) is used on the vehicle at any location where the aerodynamic, propulsion or other heating source will cause the structural temperature to be exceeded and/or the thermal stresses would be too high. A passive thermal protection system is used where possible, because it weighs less than active cooling panels with associated system weight. All of the vehicles in the current study have integral hydrogen tanks, which makes the design of the TPS especially challenging. A layer of cryogenic insulation is used under the TPS in areas directly over a cryogenic hydrogen tank. These layers of insulation must survive an extreme temperature range, providing enough insulation to protect the structure and control heat gain to the tank to minimize boil-off of hydrogen. The conditions in the tank are shown in Figure 19 for tank options of normal boiling point,

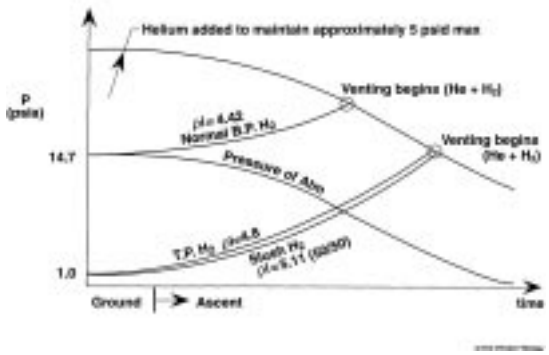

Figure 19. Tank Pressure for Hydrogen Options

triple point, and slush hydrogen.

The disadvantage of normal boiling point hydrogen is that any added heat to the tank immediately boils the liquid into a vapor. The excess pressure due to this boiling will either cause immediate venting of gaseous fuel overboard or drive up tank weights in order to contain higher pressure. Neither condition is desirable for achieving optimum vehicle performance. A super cooled fuel such as slush or triple point hydrogen is desirable for improved vehicle performance due to the reduced vapor pressure and added heat sink, which enable a lower tank design pressure and

delay the time when venting must begin. An increase in the TPS/cryogenic insulation is required to reduce the heat load to such tanks, which increases vehicle weight somewhat. However, the net effect is an advantage for the vehicle, because the slightly higher density of these liquids, over normal boiling point hydrogen, enables a somewhat greater fuel load in a given volume. Of these two fuels, slush has the marginal advantage for vehicle design due to having 50% solids in the mix, but the disadvantage of slush is that it requires a lot of ground support infrastructure and added energy costs to produce and maintain the fuel. Slush also ties flight operations to only those locations where the infrastructure is established. For these reasons triple point hydrogen is the current choice for fuel.

TPS sizing was accomplished using heat loads developed with engineering computer codes. The APAS aerodynamic panel code was used to obtain the heat loads for the airframe. Where passive TPS is not adequate, such as inside the engines, active cooling means were used. Internal engine heat loads are obtained from the 2D propulsion analysis code. These heat loads are used to perform a more detailed analysis and sizing of the cooling system and to verify the energy balance computed by the 2D propulsion analysis code. Unit weights computed from such analyses are used where active cooling is required.

Passive TPS

An advanced TPS system concept using Internal Multiscreen Insulation (IMI), shown in Figures 20 and 21 , is used on the lower surface of these

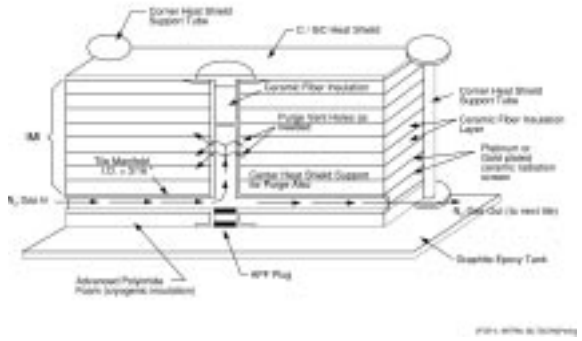

Figure 20. Internal Multiscreen Insulation (IMI) - Integrated Hot Gas Purge

configurations. A carbon silicon carbide (C/SiC)

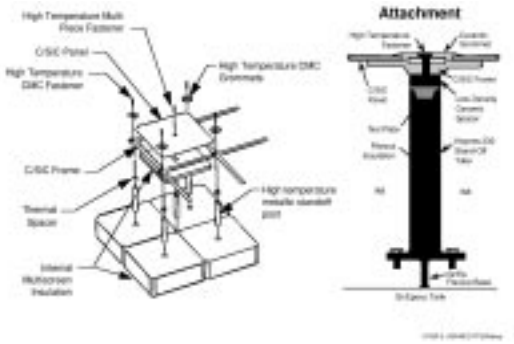

Figure 21. Advanced TPS

heat shield is used on the hot face, which has a temperature capability of 3000F. IMI is packaged beneath the heat shield and consists of layers of ceramic fiber insulation contained between layers of metallic screen. The screen resembles tissue paper in appearance. Platinum is used on the hot side because of the higher temperature capability. Gold is used toward the cold side, it has better radiation blocking performance but lower temperature capability than the platinum. This concept has a purge system integrated into the heat shield supports. The support tubes are attached directly to the graphite epoxy tank and penetrate the Advanced Polyimide Foam (APF) insulation, which is chemically bonded to the graphite epoxy tank. The foam is the cold boundary for the IMI. During ground hold, warm dry nitrogen gas is supplied through a ground support umbilical and exhausts to the atmosphere at a minimum temperature of 40F, which will prevent frost formation on the external surface. The flow rate of purge gas is sized to maintain the foam-to-IMI interface location above the liquefaction temperature of air (-298F). The continuous supply of dry nitrogen purge will also keep water vapor out of the insulation system while on the ground. Any fuel boiled off due to this heating is made up by GSE, prior to disconnect for takeoff.

Tailorable Advanced Blanket Insulation (TABI), shown in Figure 22 , is used on the upper surface of the vehicles. The upper surface has significantly less heat load than the lower, which is why TABI is the best choice. Insulation concepts that have containment systems prove to be heavy at small thickness because the heat shield and support system weights are almost independent of thickness. The TABI insulation system consists of a surface coated, fiber mat containment system with triangu-

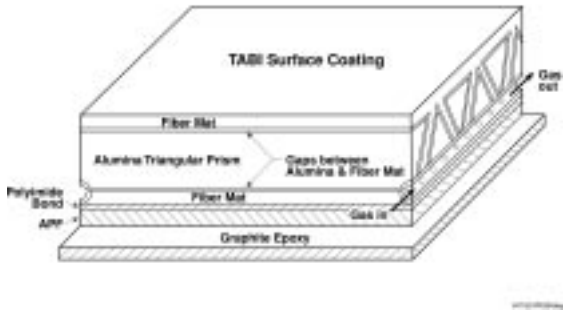

Figure 22. Tailorable Advanced Blanket Insulation (TABI) with Integrated Purge

lar, alumina prisms inside. A polyimide coating must be applied to the TABI so that it can be chemically bonded to the APF insulation. The polyimide chemical bond is important because it has a higher temperature limit (up to about 550F) than an RTV bond (up to about 400F), which was used in prior TPS concepts. The APF is also chemically bonded to the graphite epoxy tank. The graphite epoxy is limited to a temperature of 250 F, but this limit was not a controlling factor in the design. A purge gas system is integrated into the insulation to prevent liquefaction of air and frost formation while on the ground. Warm, dry nitrogen gas is circulated through the insulation system in the same manner as described above.

Passive TPS Sizing

The analysis and sizing of passive TPS was accomplished using the SINDA-85 finite difference, thermal analysis code [9]. The process uses a highly specialized set of input files containing logic for sizing of insulation based on iterative transient analysis. TPS was sized for each of the panels in the APAS aerodynamic model through an automated process that uses heat loads computed by APAS. Geometric models containing more than 1000 panels have been run for these configurations, with different analysis models used for surface locations where there is a cryogenic tank versus locations where there is no tank. The analysis model for passive TPS over a cryogenic hydrogen tank is shown in Figure 23 . The aerodynamic heat load was applied to the C/SiC heat shield on the outer mold line and the hydrogen in the tank provides a heat sink on the inside surface of the model. A transient analysis of the system was run for the complete ground hold and flight mission. The analysis started with a minimum insulation

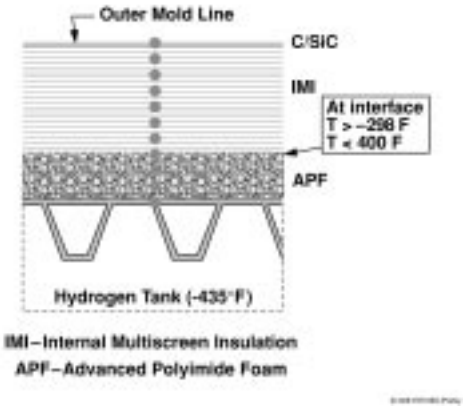

Figure 23. Analysis Model for Advanced TPS

thickness on the first iteration and proceeded to increase the insulation on subsequent iterations, until the temperature requirements of the design were satisfied. TABI and IMI were sized for the HTO SSTO mission. These results were computed on the as-drawn vehicle geometry of ABLV-4 and the unit weights applied in the vehicle closure process for all configurations. The unit weight results for the upper surface averaged 0.818 psf for the TABI and APF foam system. On the lower surface, the unit weight averaged 1.593 psf for the IMI and APF foam system. When area-averaged over all covered surface the TPS unit weight was 1.117 psf.

Active Cooling

Active cooling is used on inlet ramps, inside surfaces of the engine, external nozzle, and leading edges of the fuselage and engine inlet cowl. For these vehicles, hydrogen was used as the coolant, which flows through the cooling panels and leading edges. Cooled leading edges and cooling panels are typically made of copper alloy or high temperature super alloys such as molybdenum-rhenium or Haynes 188 alloy. Using the hydrogen fuel as a coolant enables the heat load input to the vehicle to be used regeneratively for energy to drive fuel system turbopumps. The required energy balance must be iterated between the propulsion performance code and the thermal analysis of engine cooling. The weights for cooling panels and system components used for the high-speed engines are supported by prior analyses for this mission. Mostly passive TPS is assumed for the low-speed system. However, fuel cooling will be required for some low-speed system components. A complete cooling system analysis must be performed on the final low-speed system design, in

order to size the components and balance coolant flow rates. Estimates of these component weights were used to determine the installed weight of the low-speed systems in this study.

Airframe Subsystems

The subsystems used in current airbreathing vehicle analysis are based on previous results done to a detail design level. Extensive design studies for prior vehicles yielded detailed system layouts, schematics, and master equipment lists. This work was reduced to a set of airframe system algorithms for predicting system weight and volume of the installed equipment. This data was updated during the ATS Study and scaled to operational vehicle size (fuselage volume of 100,000 ft^3). Except for some minor updates for the ABLV Study, these systems carry that same detailed design heritage into the current effort. The system requirements, vehicle sizes, and vehicle weights for the current effort are assumed to be similar enough to previous work to warrant using these data. This is further justified, based on continued similarity of system content and functionality for the current configuration.

The general arrangement of the ABLV-9 configuration is shown in Figure 24. Note the low-speed

Figure 24. ABLV-9 General Arrangement

system inlets forward of the high-speed engine and the main landing gear moved out of the sidewalls. Systems layout is described in Figure 25. Payload integration over the low-speed system is shown in Figure 26. The following sections briefly describe some of the more important airframe subsystems.

Propellant and Pressurization Systems

The fuel system utilizes triple point hydrogen for all engine modes. A schematic of the system is shown in Figure 27 . Each tank has a pressure

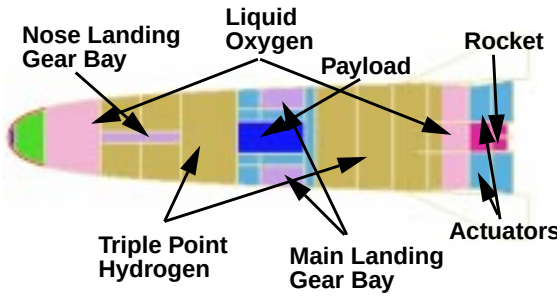

Figure 25. Systems Layout

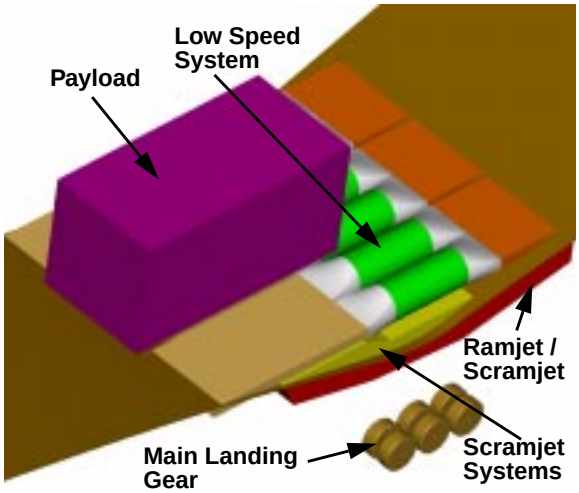

Figure 26. Payload Integration

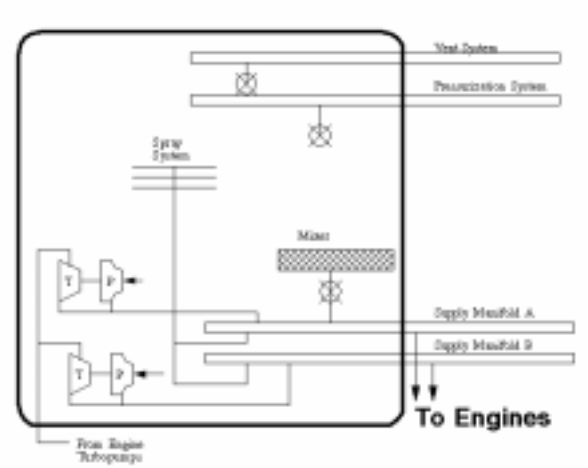

Figure 27. Propellant System

transducer, a temperature transducer, a liquid level transducer and a liquid point transducer. Each tank is also connected to a vent system manifold that controls ullage pressure. The mixer and spray sys-

tem are required to maintain a constant temperature in the tanks, in order to prevent a pressure collapse that would occur from splashing of cold liquid into a warmer ullage area. The tank turbopumps provide working net suction pressure to the main engine turbopumps, which in turn power the tank turbopumps after the system is started. The exhaust from the tank turbines is returned to the supply manifolds, along with the hydrogen supplied by the pumps.

Atmospheric oxygen is used as the oxidizer for both the low-speed engine, as well as the DMRS high-speed engine. Separate liquid oxygen (LOX) tanks are integrated into the vehicle to operate the LOX augmented scramjet mode, the linear aerospike tail rocket, and the reaction control system (RCS). The oxygen tanks are a multi-lobe, aluminum-lithium structure designed to contain liquid oxygen. The placement of the oxygen tanks is driven by trajectory requirements for CG location and control.

Pressurization and purge functions are accomplished with gaseous helium. The spherical helium tanks are located inside of the liquid hydrogen tanks to keep the stored helium at the highest possible density. The hydrogen tanks are pressurized by helium to only 5 psig at the beginning of the mission, while the LOX tanks are run at about 35 psig. Additional helium is admitted to the tanks as liquid is removed, to maintain pressurization. However, as the tanks are heated the vapor pressure of the hydrogen or LOX rises and less and less helium is required for pressurization. Careful control of the heat load on the tanks is required to limit boiloff, but increased thickness of TPS must be carefully evaluated as it reduces overall volume available within the vehicle.

Actuation and Hydraulics

The hydraulics system controls both discrete and continuously varying operations on the airframe. The discrete operation includes the actuation of the landing gear, while continuously varying operations include actuation of the horizontal and vertical control surfaces. Hydraulics also control wheel brakes and nosewheel steering. The actuators for the control surfaces are shown in Figure 28.

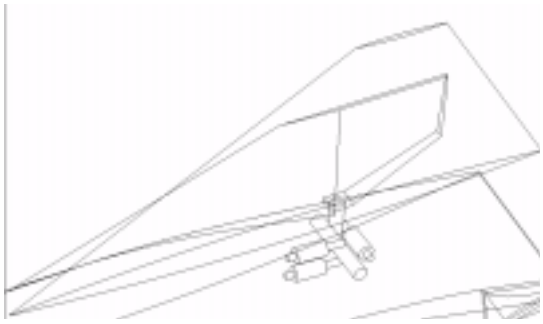

Figure 28. Control Surface Actuators

Landing Gear

The design drivers for the landing gear are the volume required in the vehicle, the takeoff speed, the vehicle weight, and the tipback angles. The general arrangement of the landing gear is depicted in Figure 29.

Figure 29. Landing Gear Arrangement

Tires and landing gear carriages occupy a large volume that must be placed inside the fuselage near the gear attachment points. The takeoff speed of SSTO vehicles is extremely high, approaching three hundred knots. This requires a structure and a system that can withstand these high speeds and drag forces, while loaded at maximum TOGW. Landing at vehicle empty weight (with payload) is not considered a design driver during conceptual design, because other conditions, such as taxi bumps at maximum TOGW, have been shown to be a greater structural challenge. The tipback angle typically chosen for these configurations is fifteen degrees, allowing a 14 degree AOA with some margin at takeoff.

Vehicle Synthesis

It is highly unlikely that the vehicle design team will pick a vehicle size that provides the precise PFA to perform a required mission. Therefore, a means is needed to resize the vehicle to the mission required size. This process must be something other than redesigning and reanalyzing the vehicle over and over (trial and error). The ideal process would take into account complex multi-discipline interactions and non-linear effects of chang-

ing propulsion and internal system sizes. It would also accommodate changes in mission requirements and trajectory refinement, as well as model all sorts of physical relations and accept a variety of multi-discipline information.

This ideal process does not exist, but the authors have evolved a process that synthesizes a vehicle design from an assembly of its constituent parts and systems. Vehicle synthesis connotes a modeling process that collects individual math models of the vehicle components, each modeled as a function of size or other physical quantities related to size, such as thrust or power. All components are reduced to an algorithm or series or equations to describe its weight and volume occupied. Each of the individual models is linked to the geometry model of the vehicle so that changes in surface areas and volumes are known to the collective process. The entire model is implemented on a multi-page workbook (assembly of spreadsheets) for ease of communication between sections. The set of equations is highly interactive and must be solved by iteration, so the spreadsheet format is ideal to track nearly a hundred individual items.

The assembly of this model involves expert input from the multi-discipline team. The spreadsheet format allows ready access to all models and makes updates simple and easy, as each discipline matures its design input. Another interesting feature of this format is the ease of performing trade studies. Quick changes of models or technology features can easily be implemented for comparison of impact on the closure weight. The interaction of the team members during its construction is one of the keys to an accurate vehicle assessment. Changes in sizing are driven by photographic scaling from a reference size. From the trajectory analysis, a PFR and average propellant density are computed. The average propellant density is directly related to LOX fraction and was easier to implement in the synthesis. These values are input to the tool and it iterates until a closure is obtained. For the work in this paper, the synthesis model was indexed to a fuselage volume of 100,000 ft^3, which necessitated small adjustments in input parameters from those of the as-drawn vehicles, with fuselage volumes around 120,000 ft^3. These minor adjustments were likewise made by photographic scaling. Thus, all sub-models or algorithms in the synthesis tool were accurately indexed to a common fuselage volume of 100,000 ft^3. The synthesis tool also provides useful information and guidance to the design team in performance of the analyses and design task. The tool keeps track of propellant fraction, LOX fraction, mass properties, CG location, and load distribution as a function of fuselage station. This information is used in trajectory simulation, structural analysis, and weight prediction.

The synthesis process works very well for photographic scaling because small changes in size don't affect aerodynamic coefficients and propulsion efficiencies. Thus, gross thrust, lift, drag, and pitching moment will scale accurately to the second power of photographic scale factor, for small changes. The size of the as-drawn vehicle must be carefully estimated because all aerodynamic and propulsion analysis will be performed on geometric models derived from the original as-drawn configuration. A critical issue for closure accuracy becomes the magnitude of the closure scale factor. Every model in the synthesis process was based on point-design information at the as-drawn size. If the models had been based on a very small fuselage volume the uncertainty (error) in scaling to a much larger volume would be greater. The goal for this effort was to keep closure scale factors within 10% of the reference size. Thus, the choice of an as-drawn size for the point design work is important, both to performance analyses and design work. If the propulsion integration performs so poorly that the vehicle PFR drives the closure scale factor out of range, then there are several potential areas of concern. The least of these is the error caused by scaling. Although the error will increase as scale factor moves out of the desired range, the trends will still hold. The more relevant concern is to understand the fundamental problem with the configuration. Immediate areas to focus on would be cycle performance, installation penalties, aerodynamics, and vehicle drag including trim effects.

Closure

The closure process brings all relevant design and analysis data together in the synthesis model. For a particular LOX fraction, the PFA may be determined from the synthesis model independently of mission performance information. This may be represented as a continuous curve of PFA vs. TOGW as shown in Figure 30 for the status ABLV-9 vehicle. Every different LOX fraction will produce a different curve, so in reality there will be a family of curves. From the trajectory simulation a PFR and LOX fraction are determined to fly the

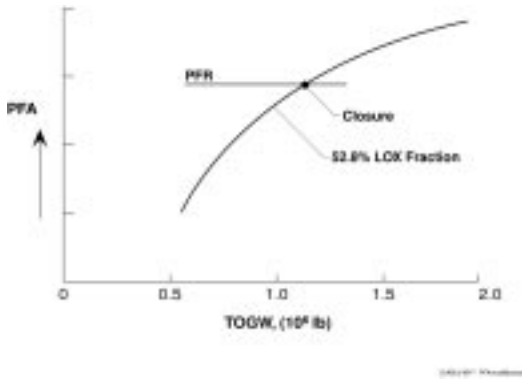

Figure 30. PFA vs. TOGW Closure Curve

mission. The closure process may be visualized as selecting the correct LOX fraction curve and picking the TOGW that corresponds to the required PFR. Note that the LOX fraction and PFR are linked through the trajectory simulation, so vehicle comparisons on the basis of PFR alone can be quite misleading. Recall that the figure-of-merit selected for this study was minimum TOGW. Vehicle DW may be treated in the same manner and will exhibit similar trends.

Before moving to the closure details, a discussion of design maturity and analysis fidelity is in order. All of the vehicle designs in this paper are relatively mature and the analysis methods are at a consistent level. All trajectory simulations were 3DOF with aerodynamic trim in the pitch plane. Aerodynamic databases were based on consistent engineering methods, CFD, and wind tunnel testing. Propulsion performance was based on 2D methods for inlets and nozzles, with 1D combustor cycle codes, both for low-speed and high-speed engines. The low-speed cycle code was P&W proprietary and the high-speed combustor model is extensively validated against actual wind tunnel data for numerous engine models. Recall that no 3D effects were taken into account in the propulsion performance for any vehicle. The impact of 3D effects on the propulsion is more relevant in the scramjet mode and must eventually be assessed in the configuration development. However, the substantial CFD effort required to assess inlet and nozzle effects at multiple Mach numbers preclude its use in multiple configuration studies. Internal packaging and subsystems layout were performed with 3D CAD tools. Structures and TPS were based on prior analysis and were consistent for all configurations. Installation weights for the turbine engines were estimated based on previous design studies, but were increased by 20% for the ABLV-9B vehicles because of the added variable geometry. All CTSC configurations used triple point hydrogen fuel. Based on the relative scale illustrated in Table1, the results presented herein are at a

Table 1: Design Maturity Level

Design Maturity	Color Code	Propulsion	Aero	Structure Weight	Vehicle Performance	Synthesis & Packaging
10	Blue	Flight Data	Flight Data	Flight Vehicle	Flight Vehicle Performance	Flight Vehicle
9	Light Blue	Wind Tunnel Data	Wind Tunnel Data	Components Fab/Test	6 DOF Hardware Simulation	Mock-up, CAD Multi-Exp. Non-Linear
6	Green	CFD Certified	CFD Certified	FEM Certified	6 DOF/ 6 DOF Trimmed	CAD Multi-Exp. Non-Linear
5	Light Green	Cycle Certified	Engineering Methods Certified	Unit Loads Certified	3 DOF Trimmed	CAD Multi-Exp. Non-Linear
3	Yellow	CFD Uncertified	CFD Uncertified	FEM Uncertified	3 DOF unbalanced	Single Exp., Non-Linear
1	Orange	Cycle Uncertified	Engineering Methods Uncertified	Unit Loads Uncertified	Energy State	Single Exp. Linear
0	Red	Tabral Cycle	L/D, Cd Estimated	Design Tables	Rocket Equation	Estimated

design maturity level of 5 or 5+. An important consideration in vehicle development is weight growth as the design matures. To provide added margin in the TOGW predictions made by the closure process, the synthesis tool includes a 15% DW growth allowance imposed above the predicted values of vehicle DW. This penalty is imposed on all individual components of the vehicle in a continuous manner to assure that all closure TOGWs allow for continued dry weight growth at lower design maturities. The growth factor should be reduced as the vehicle reaches final design.

Figure 31 shows the status TOGW across the

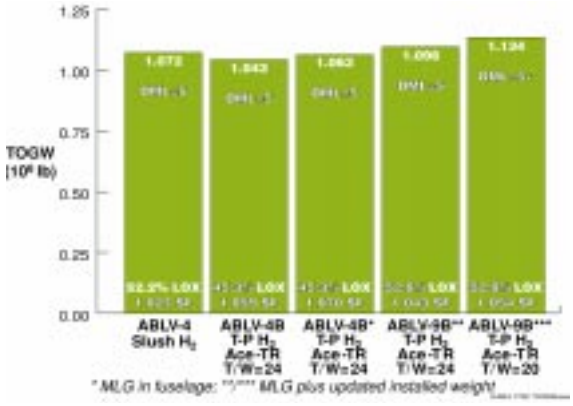

Figure 31. TOGW of Configurations

configurations analyzed in the current study. On the left is the reference vehicle ABLV-4 at 1.07×10^6

lb., followed by the first Ace-TR derivative, ABLV-4B at $1.043x10^6$ lb.(old MLG installation) and the ABLV-4B* at $1.063x10^6$ lb. (*MLG in fuselage). The next vehicle is ABLV-9B** at $1.096x10^6$lb. (Ace-TR T/W=24 and updated installation weights), followed by the final configuration, ABLV-9B*** at $1.134x10^6$ lb. (Ace-TR T/W=20 and updated installation weights). An important criteria for evaluation of these results is the current runway weight limit for an HTO configuration. This is estimated to be about $1.25x10^6$ lb. for the current runway construction. With the 15% dry weight growth factor included in these results, an acceptable margin exists for this limit.

Figure 32 depicts DW for the same configurations. Note that the DW of the ABLV 4B* configuration is higher than the ABLV-9B**, but recall that the body width of ABLV-4 allowed integration of eight (8) Ace-TR engines, while the more slender ABLV-9B** housed only six (6) Ace-TR engines. With only six engines, the ABLV-9B** configuration had less thrust and required more rocket augmentation in the low-speed range, which slightly increased LOX use and TOGW, but still had lower DW due to only six Ace-TR engines. The ABLV-4B configurations, with eight Ace-TR engines, had more thrust and required less rocket augmentation in low-speed, delivering slightly lower LOX use and TOGW. However, the eight Ace-TR engines drove up the DW. In this case, the slightly higher TOGW may be desirable, in order to reduce cost of the low-speed engine installation (six engines vs. eight).

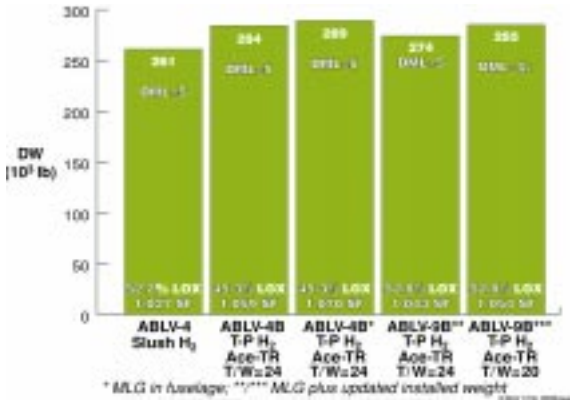

Figure 32. Dry Weights for Configurations

Summary and Conclusions

The development of a promising HTO SSTO configuration was traced through the multi-discipline design and analysis process. The mission and trajectory development were described along with the aerodynamic and propulsion predictions supporting the 3DOF simulation. The propulsion-airframe integration of both low-speed and high-speed propulsion systems was described, from both aero-propulsive and mechanical perspectives. Design details of the preferred configuration were described, along with the supporting analyses performed to substantiate the status results. Vehicle packaging was described and mechanical designs were disclosed, with structures, materials, and technologies employed. Finally, the closed vehicle weights were provided.

Particular attention was focused on describing the complex multi-discipline process as the preferred configuration was developed. The maturity of the design and analysis was discussed and assessed on a relative scale, which was provided to illustrate the differing levels of credibility achieved with various design/analysis approaches. With reference to Figure 40, the final ABLV-9B*** configuration is assessed a Design Maturity Level of 5+. The CTSC concept appears to be a robust propulsion system with good potential for real vehicle development. There was some weight growth, relative to the ABLV-4 reference vehicle, as the new configuration was moved through this study. However, there was a substantial payoff in design credibility with that growth. Slush hydrogen was removed from the vehicle to reduce infrastructure costs. The main landing gear were moved into a more conventional fuselage integration, substantially reducing risk from the reference installation. An updated weight estimate was imposed on the Ace-TR installation and the uninstalled T/W was reduced from 24 to 20.

However, there are many additional areas that should be worked to further mature this design. The updated structural analysis capability needs to be completed and factored into the closure. The synthesis tool update needs to be enhanced to take advantage of the new structural capability. A higher fidelity design study of the low-speed inlet and nozzle should be performed to better predict installed weight and volume for optimization of the ramjet takeover Mach number. Fuel cooling of low-speed inlet flow should be explored to see if the

engines could be downsized to save weight and volume. The impact of fineness on low-speed system installation should be explored to exploit any possible cost advantages. Additional turbine-based engines should be assessed against the Ace-TR to see if one may have an advantage. When a more optimum configuration is ready, the 3D propulsion effects should be assessed. Low-speed inlet and nozzle performance should be reviewed to assess whether they might be improved.

In conclusion, the current study has identified and assessed a promising configuration for the HTO SSTO mission. The lifting body with CTSC airframe-integrated propulsion is supported by many years of research, design, analysis, and experimental results for the key technologies. The current configuration offers potential for further development and optimization. The propulsion and airframe technology incorporated in this vehicle should be supported with continued research and hardware demonstration, to provide the enabling technology for the next century's revolutionary flight vehicles.

Acknowledgments

The authors wish to express their sincere appreciation to A. M. (Jose) Espinosa of The Boeing Company in St. Louis, MO, for his substantial contribution in supplying the installed low-speed system performance for these studies. The authors also wish to thank Hilmi Kamhawi for his AML programming support, which enabled much improved productivity for 2D propulsion analyses. Finally, the authors must acknowledge Charles R. McClinton of NASA Langley Research Center for his continued support of the tool and process development necessary to perform this complex work.

References

1). McClinton, C.R., Hunt, J.L., Ricketts, R.H., NASA Langley Research Center; Reukauf, P., NASA Dryden Flight Research Center; Peddie, C.L., NASA John Glenn Research Center; "Airbreathing Hypersonic Technology Vision Vehicle and Development Dreams", AIAA 99-4978, November 1999.

2). Hunt, J.L., "Airbreathing / Rocket Single-Stage-to-Orbit Design Matrix", AIAA 95-6011, April 1995.

3). Adaptive Modeling Language, Version 3.1.2, TechnoSoft, Inc. Cincinnati, OH. Copyright 1999.

4). Pro/ENGINEER, Release 9839, Version 20, Parametric Technology Corporation, Waltham, MA, Copyright 1988-1998.

5). Powell, R. W. et al, NASA LaRC, Brauer, G. L. et al, Lockheed Martin Corp., "Program to Optimize Simulated Trajectories (POST) Version 1.03", February 1998

6). Sova, G., Divan, P., "Aerodynamic Preliminary System II", North American Aircraft Operations, Rockwell International, Los Angeles, CA.

7). Gentry, A. E., Smyth, D. N., Oliver, W. R., "The Mark IV Supersonic-Hypersonic Arbitrary-Body Program", McDonnell-Douglas Corporation, Technical Report AFFDL-TR-73-159, November 1973.

8). Collier, C.S., "HyperSizer Analytical Methods & Verification Examples", Collier Research Corporation, 1998.

9). Cullimore, B. A., Ring, S. G., Johnson, D. A., "SINDA/FLUINT General Purpose Fluid Network Analyzer, Version 4.1", Cullimore and Ring Technologies